Swiss J Geosci (2014) 107:101–112
DOI 10.1007/s00015-014-0161-0

2D geological–geophysical model of the Timok Complex (Serbia, SE Europe): a new perspective from aeromagnetic and gravity data

Snežana Ignjatović · Ivana Vasiljević · Milenko Burazer · Miodrag Banješević · Ivan Strmbanović · Vladica Cvetković

Received: 26 August 2013 / Accepted: 21 May 2014 / Published online: 19 June 2014

Abstract The study reports new aeromagnetic and gravity data for the northern part of the Timok Magmatic Complex (TMC), East Serbia. The TMC is part of the Tethyan Eurasian metallogenic zone well known for hosting large copper and gold deposits. The complex formed by continuous volcanic activity 90–78 Ma ago, that developed in roughly three phases: Turonian andesites, Santonian–Campanian andesites/basaltic andesites (both mostly volcanic) and Campanian latites/monzonites (mostly shallow intrusive). The aeromagnetic measurements included acquiring total magnetic intensity data that were corrected for diurnal variations, leveling, microleveling, calculated normal field values, calculated anomaly values of total magnetic field intensity and reduction to the pole. The gravity measurements were carried out in an irregular grid with relative gravity values obtained using a Worden gravity meter. 2D modeling reveals that the subsurface extension of the Campanian Valja Strž pluton is ten times larger than it is indicated by its surface outcrops. This implies that the area south and southeast from the pluton can be interesting in terms of finding new porphyry systems. The model indicates that this intrusive body should not be considered as a deeply dissected pluton. This sheds new light onto its potential with respect to epithermal gold mineralization, as well. The model also suggests that there are larger non-exposed bodies of Santonian–Campanian volcanics and near-surface hydrothermally altered rocks than it is inferred from geological maps. The results of our study suggest that further interdisciplinary investigations in the TMC, in particular those integrating geophysics and geology, may have potential of advancing the existing exploration models.

Keywords Banatitic belt · Geophysical survey · Copper deposits

Editorial handling: E. Gnos.

Electronic supplementary material The online version of this article (doi:10.1007/s00015-014-0161-0) contains supplementary material, which is available to authorized users.

S. Ignjatović · I. Vasiljević · V. Cvetković (✉)
Faculty of Mining and Geology, University of Belgrade, Đušina 7, 11000 Belgrade, Serbia
e-mail: cvladica@rgf.bg.ac.rs

M. Burazer
NTC Geophysical Department, NIS-Naftagas, Batajnički drum 18, 11000 Belgrade, Serbia

M. Banješević
Technical Faculty in Bor, University of Belgrade, Vojske Jugoslavije 12, 19210 Bor, Serbia

I. Strmbanović
Avala Resources Ltd, Studentski trg 4, 11000 Belgrade, Serbia

1 Introduction

The Timok Magmatic Complex (TMC) belongs to the East Serbian Carpatho-Balkanides which is part of the Tisza-Dacia Unit. The Tisza-Dacia Unit acted as the western margin of the European plate during the last subduction processes that were associated with the final closure of the last Tethyan realms in this region (e.g. Schmid et al. 2008, and references therein). The TMC is geographically situated in East Serbia and occurs as a 60 km long and almost N–S stretching area. The complex continues northward to Romanian Banat and southeastward to Srednogorie in Bulgaria, thereby forming a regional zone (see inset of Fig. 1) known as Banatitic Magmatic and Metallogenic

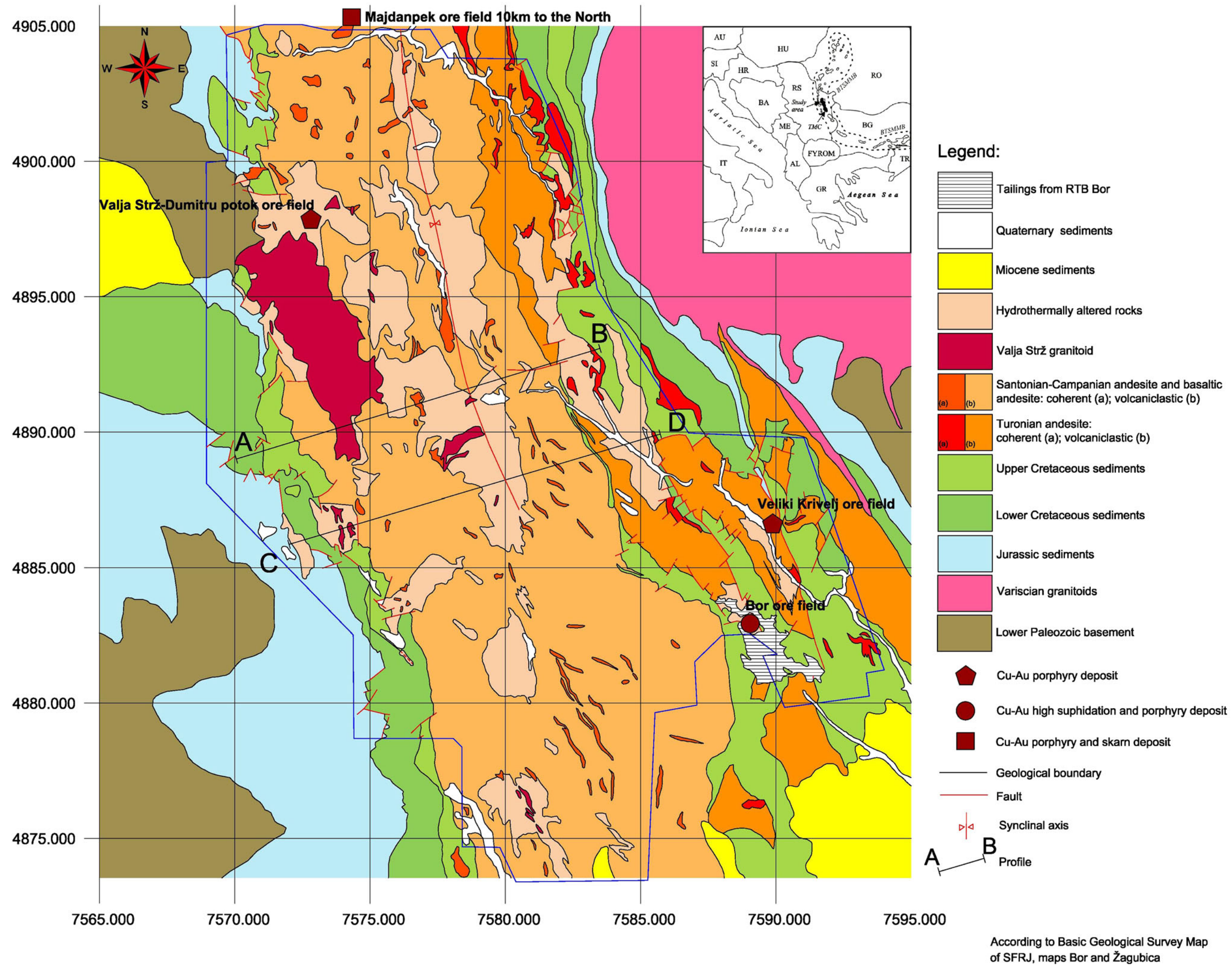

Fig. 1 Geological map of the study area (with the position of sections *AB* and *CD*)

Belt (Berza et al. 1998; Ciobanu et al. 2002) or Apuseni–Banat–Timok–Srednogorie belt (Mitchell 1996). Because it hosts some of the most significant copper deposits in Europe, the Banatitic Magmatic and Metallogenic Belt is important part of the Tethyan Eurasian metallogenic zone (Janković 1990).

The Timok Magmatic Complex is one of the largest volcanic regions in Serbia and is surely the most important one in terms of ore deposits. It is generally composed of large piles of Upper Cretaceous andesitic volcanic and volcaniclastic rocks, which are cut by numerous porphyritic dikes and a few relatively larger plutonic bodies (Karamata et al. 1997; Banješević 2006). The TMC magmatism exhibits a typical calc-alkaline character and is characterized by a pronounced westward age progression (Kolb et al. 2013), which is in agreement with a southward shift in age observed in Bulgarian Srednogorie (von Quadt et al. 2001; Stoykov et al. 2004). This age pattern is interpreted as the consequence of the rollback of eastward (northward in Bulgaria) subduction (e.g. von Quadt et al. 2005; Lips 2002; Zimmerman 2006; Zimmerman et al. 2008). Both porphyry- and skarn type deposits are known to occur in the TMC, and four areas are delineated as most important (e.g. Zimmerman et al. 2008): (1) Majdanpek porphyry-skarn deposit occurring in the far north, (2) Veliki Krivelj Cu-porphyry system situated towards the southeast, (3) Bor Cu–Au–Mo deposit characterized by porphyry to epithermal mineralization, and (4) Valja Strž plutonic complex and associated Dumitru Potok Cu porphyry system, which occur along the western margin of the complex.

During the last several decades large amounts of geological information have been acquired regarding the origin and evolution of the TMC and the links between tectonomagmatic and ore forming processes (see Bor's 100th anniversary publications: Janković et al. 2002; Koželj

2002; Koželj and Jelenković 2001, and references therein). These geological studies have supported a more than a century long exploitation with reported historical production of 6 million tonnes of copper and 300 tonnes (9.65 million ounces) of gold (Monthel et al. 2002). This exploitation relied upon relatively old geological knowledge, i.e. it was mainly based on deposits that had long been known to exist. On the other hand, most geological studies of the last decades were predominantly aimed at increasing the resolution of the age data (von Quadt et al. 2002, 2003, 2007; Lips et al. 2004; Clark and Ullrich 2004; Banješević et al. 2006; Zimmerman et al. 2008; Kolb et al. 2013), reconstructions of volcanic facies (Banješević et al. 2001, 2002), and only some of them had more direct bearings on the local patterns of mineralization and surrounding hydrothermally altered rocks (Pačevski et al. 2007, 2008, 2012).

In the last couple of years this world-class copper mining district entered a new and very exciting phase of geological explorations. The results reported by Reservoir Minerals Inc and Freeport McMoRan about the Hole FMTC 1210, which indicate the presence of a blind high sulphidation and porphyry copper–gold mineralization beneath the post-mineralization Miocene cover sediments (http://www.northernminer.com/news/reservoir- freeport-hit-high-grade-copper-at-timok/1001679498/), as well as new porphyry Cu–Au prospects that were found in the western part of the TMC around the Valja Strž pluton (Avala Resources Ltd.), suggest that there is still a lot to uncover in this ore-bearing complex. These recent results have encouraged further geological studies, in particular those aimed at integrating geophysical surveys and traditional geological investigations. In this paper we report and discuss so far unpublished results of aeromagnetic and gravity measurements for the northern part of the TMC. The investigations were primarily aimed at determining the location of unexposed magmatic bodies and their spatial relationships with the surrounding rocks. We believe that this study brings important steps forward in our present understanding of the geological structure of the TMC. This, in turn, can provide new prospectives for ore explorations in this area with better chances of assessing the controls on distribution of still undiscovered porphyry Cu (±Au–Mo) and epithermal Au–Ag deposits.

2 Geological setting

The Timok Magmatic Complex developed onto a continental basement composed of various rocks that range in age from the late Proterozoic to Early Cretaceous (Andrić et al. 1972; Antonijević et al. 1974). The basement belongs to the Getic nappe of the Dacia Unit and is represented by medium- to high-grade metamorphic Neoproterozoic to Early Palaeozoic gneisses and sub-greenschist to epidote–amphibolite grade Palaeozoic rocks (Krstić and Karamata 1992). This series is intruded by numerous Variscan granitoids (323–306 Ma; Vasković et al. 2012) and is overlain by Late Paleozoic clastic sediments as well as by Early Cretaceous carbonate sediments. The overstep sequences, which clearly postdate the mid-Cretaceous nappe stacking of the Austrian phase (Săndulescu 1984), are predominantly composed of Cenomanian molasse-like sediments.

The TMC formed by continuous volcanic activity during the period of around ten million years, roughly between 90 and 78 Ma (von Quadt et al. 2002; Lips et al. 2004; Clark and Ullrich 2004; Zimmerman et al. 2008; Kolb et al. 2013). During this evolution the volcanic front continuously migrated from the east to the west (von Quadt et al. 2002, 2003, 2007). The available geochronological data indicate that the volcanism began in the Turonian after the Albian–Cenomanian transgression that was characterized by deposition of clastic sediments overlying Barremian–Aptian limestones or/and carbonaceous sandstones. The Turonian volcanic products are subaerial extrusive to subvolcanic rock facies mainly of andesite and subordinately dacite compositions. Both the Albian–Cenomanian sediments and the Turonian volcanic rocks predominantly occur along the eastern margin of the TMC (Fig. 1). The Turonian phase was followed by the formation of a new sedimentary cycle. This cycle started with sediments containing Lower to Middle Turonian microfauna (Ljubović-Obradović et al. 2011), and was immediately followed by a Santonian–Campanian volcanic phase. The products of Santonian–Campanian volcanism developed in the western part of the TMC and were predominantly represented by andesite to basaltic andesite extrusions that very often emplaced in subaqueous environments. At the same time, the whole TMC acted as an elongated deposition space which eastern and western parts had different evolution (Đorđević and Banješević 1997). The sedimentation in the eastern part was characterized by deposition of reworked volcaniclastic rocks until the Maastrichtian, whereas in the western block fine-grained flysch-like sediments deposited until the Middle Santonian. The TMC magmatism ended by the emplacement of Campanian intrusions and dikes of predominantly latitic to trachyandesitic compositions. These magmatic bodies are commonly found cutting the westernmost part of the TMC. The largest intrusion is the Valja Strž monzonite pluton which is situated at the westernmost margin of the TMC (Fig. 1). The sedimentary processes continued until the latest Maastrichtian, when reef carbonates and coarse-grained and regressive clastites were deposited.

3 Results

3.1 Data acquisition

Geophysical data comprise aeromagnetic and gravity measurements carried out in different time and for different purposes. The studied region is situated in the northern TMC and covers an area between 7,568,600 and 7,594,000 m and between 4,874,570 and 4,905,300 m in Gauss–Krüger coordinate system (see rectangle in Fig. 1).

3.1.1 Aeromagnetic data

The aeromagnetic survey was done in 2006 by "Dundee Precious Metals Inc." (now "Avala Resources Ltd."). The measurements were carried out by "Geotech Airborne Ltd." (Geotech) by utilizing "Geometrics" optically pumped caesium vapour magnetic field sensor. The sensor was mounted 15 m below the helicopter. The sensitivity of the magnetic sensor was 0.02 nT at a 0.1 s sampling interval. The helicopter position was maintained 90 m above the ground along the lines with 50 and 100 m line spacing. The helicopter was flying in SW–NE direction, i.e. perpendicularly to the direction of the major geological structures that occur in the study area. Total Magnetic Intensity (TMI) data were acquired from aeromagnetic measurements. The processing of magnetic data involved corrections for diurnal variations, leveling, microleveling, calculated normal field values, calculated anomaly values of total magnetic field intensity and reduction to the pole.

The TMI data were corrected for diurnal variations by using digitally recorded ground base station magnetic values. Tie line leveling was done by adjusting intersection points along traverse lines, and after that the microleveling procedure had been applied. Microleveling adjustments are necessary because even quite minor data errors become clearly visible when data grids are displayed as enhanced images. This technique is designed to remove persistent low-amplitude components of the flight line noise, which remain after tie line leveling (Luyendyk 1997). Normal field values were calculated by means of model IGRF-11 (International Geomagnetic Reference Field) for the period of the aeromagnetic measurements. Anomaly values of the intensity of total magnetic field were calculated as differences between measured magnetic field and calculated normal field values. The magnetic anomaly data were converted to a 50 m grid using kriging technique. Because of dipolar nature of the magnetic field, prior to data interpretation a procedure of reduction to the pole (RTP) was applied. The RTP technique transforms all magnetic anomalies into anomalies that would be measured at the north magnetic pole (Cooper and Cowan 2005; Li 2008). This technique makes the shape of magnetic anomalies better reflecting the spatial location of geological structures that are responsible for the anomalies (hereafter referred to as *source structures*). Furthermore, the transformation ensures that anomaly maxima are located centrally over these structures (Salem et al. 2007). The aeromagnetic data were reduced to the pole using magnetic inclination and declination of 61° and 4°, respectively, which corresponds to the geomagnetic field at the time of the aeromagnetic measurements. The total magnetic field anomaly map reduced to the pole is given in Fig. 2.

3.1.2 Gravity data

Detailed gravimetric surveys in Serbia were performed during a relatively long period between 1952 and 1984 and most of the measurements were carried out by the Geophysical Institute Belgrade. During this period, first and second order gravimetric networks were completed. Along with the permanent establishment of the reference gravimetric networks, a detailed gravimetric survey was also done. The gravity measurements were done in an irregular grid, whereas relative gravity values were obtained using Worden gravity meter. Average density of gravity stations in the survey area was 1 station per square kilometre. The gravity data contain: number and Gauss–Krueger coordinates of the points, elevation, measured gravity values, terrain corrections (estimated within a diameter of 20 km), and normal field values calculated using the formula of Cassinis (1930). The Bouguer anomaly map (Fig. 3) was done using a density value of 2.67 t/m^3 and by converting the Bouguer anomaly data to a 500 m grid.

3.2 Data interpretation

Two distinct zones having positive magnetic anomaly values and displaying almost the same NNW–SSE strike are visible in Fig. 2. The western zone consists of two positive anomaly subzones that are separated by a contact area which can be interpreted as a fault. The maximal anomaly values in this zone exceed 1,500 nT. The anomaly is most likely caused by the presence of the ~80 Ma Valja Strž granitoid (von Quadt et al. 2002; Kolb et al. 2013). The shape and size of the anomaly suggest that this pluton exists underneath adjacent sediments, i.e. that it occupies an area larger than it is apparent from its surface exposures. In the central part of the studied area there is a zone with positive anomaly values that range 100–1,000 nT. It consists of three spatially separated anomaly subzones. The source structures of these anomalies are most probably volcanic and subvolcanic rocks that are overlain by sedimentary deposits and have only smaller masses exposed on the surface (Fig. 1). In-between the high magnetic anomaly zones an area characterized by low anomaly values can be

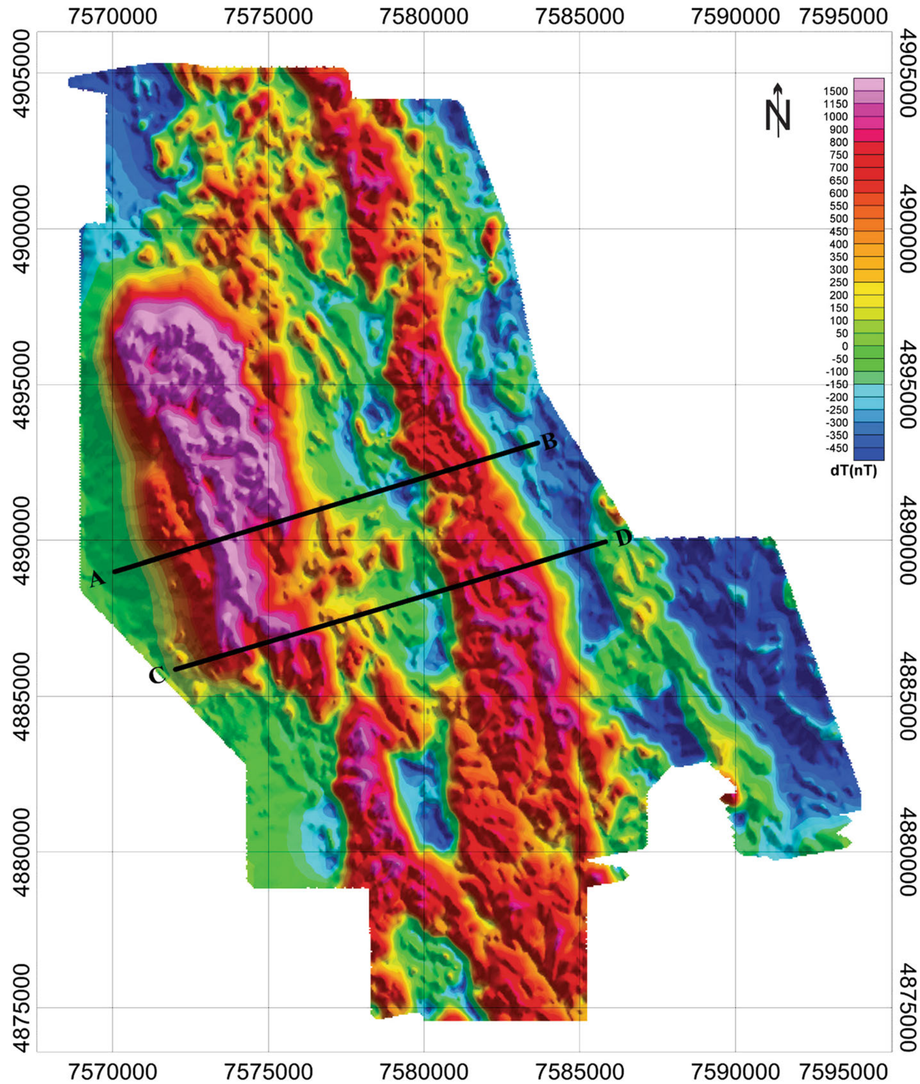

Fig. 2 Map of magnetic field anomaly reduced to the pole (RTP) (with the position of sections *AB* and *CD*)

observed. This part of the terrain is composed of hydrothermally altered rocks which protolihs are Santonian–Campanian sedimentary, volcanic and volcaniclastic rocks. In addition, low anomaly values are also characteristic for the easternmost part of the study area.

The Bouguer anomaly map reveals the presence of an anomaly zone located in the western part of the studied area (Fig. 3). The anomaly is characterized by mutually alternating local maxima and minima with amplitudes ranging between -8×10^{-5} and 11×10^{-5} ms^{-2}. The size and shape of the anomaly imply that it likely resulted from complex source structures. The western part of the anomaly is most probably caused by the Valja Strž pluton. This is in agreement with the above presented aeromagnetic data that already suggest that there is a continuation of this pluton beneath overlying sedimentary rocks. The eastern part of the anomaly is likely caused by the presence of volcanic and/or volcaniclastic rocks formed during the Santonian–Campanian volcanic phase. In addition, there is a large zone of negative gravity covering the central part of the study area. This zone consists of two gravity anomalies that are separated by a contact zone. The anomaly values range between -1×10^{-5} and -8×10^{-5} ms^{-2}. In this areas Turonian and Santonian–Campanian sedimentary and magmatic rocks are exposed. The shape, size and anomaly values indicate that this may have resulted from the presence of magmatic rocks overlain by sedimentary deposits. Between this zone and the zone in the western part of the study area there is an abrupt change in amplitude of gravity values. This suggests that two environments with contrasting density are juxtaposed and the contact between them can be interpreted as a fault. In the eastern part of the study area occurs a zone where stripes with positive and negative anomalies ranging between -1×10^{-5} and 6×10^{-5} ms^{-2} are alternating. The terrain in this area is composed of sedimentary rocks and the above mentioned

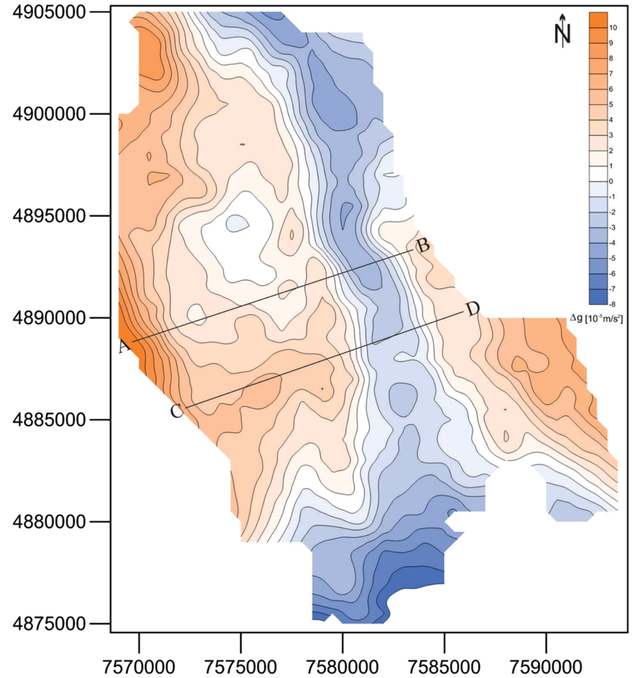

Fig. 3 Bouguer anomaly map (with the position of sections *AB* and *CD*)

anomalies most likely imply the presence of igneous rocks in depth.

4 Discussion

The method of 2D geomagnetic and gravity modeling was used for creating geological–geophysical models shown in Figs. 4 and 5. This method is applied for the source structures that are elongated in one direction, which is also the main direction of the Timok Magmatic Complex. The sections AB (14.2 km) and CD (14.4 km) are positioned perpendicular to the strike of the source structures (Fig. 1) and they cross through the most distinctive geophysical anomalies in the studied area (Figs. 2, 3).

4.1 Geophysical modeling

The basic goal of the 2D geophysical modeling was to better constrain the inferred magmatic bodies by defining their shape and extent more into detail. The modeling was done using software package Oasis Montaj, which encompasses the application for 2D modeling ("GM-SYS"). This method offers the possibility of making complex models involving a large number of geological units of different physical properties. All blocks in the model are assumed to have semi-infinite extents in direction perpendicular to the modeled section, and that is the major limitation of the method. The intensity of

Fig. 4 2D geological–geophysical model along the section *AB* with graphics of tilt derivative (TDR), aeromagnetic anomaly (ΔT) and gravity anomaly (Δg) ▶

geomagnetic and gravity anomalies is influenced by the variation in shape of source structures in the proximity of the section. The impact of these variations has been taken into account in the course of modeling.

Along with the above presented aeromagnetic and gravity maps, Basic Geological Map 1:100,000 of the study area (Antonijević et al. 1968, 1974) and available data for rock density and susceptibility were used for modeling. A gravity and magnetic 2D model represents density and susceptibility distribution along the given sections with the present lithological units are considered as equi-density and equi-susceptibility blocks. The models correspond to geological formations present in the geologic map (Fig. 1) only for those lithological units that display high contrasts in density or susceptibility. By contrast, lithological units of similar density and susceptibility were merged and presented together.

The parameters for the models of the individual sections were derived from earlier geophysical and geological surveys, including drillholes located in the proximity of the sections. These data are provided by the company "Avala Resources" and include lithology, density and magnetic susceptibility from 8 drillholes ranging in depth 200–570 m. They reveal that magmatic rocks show almost negligible variations in density but are very variable in susceptibility, hence, for modelling we adopted the average susceptibility and density values of drilled samples. Susceptibility and density of the basement rocks and sediments were determined mostly using the values for analogous rock types, which are available in literature.

The first step was modeling of magmatic rocks. Analytic signal (AS) and tilt derivative (TDR) techniques were applied for determining the horizontal edges of source structures that caused the above described magnetic anomalies more accurately. In order to define source structures which have regional significance, the upward continuation technique was used, and for refining their shape a combination of upward continuation and TDR was applied (For more details see electronic supplement).

In order to define the maximal width of the inferred magmatic bodies, we used the results obtained by the procedures of upward continuation and upward continuation with TDR, both for levels 500 m. The obtained maps show that *magmatic rocks 1* and *3* (Figs. 4, 5) are wider in extent than *magmatic rocks 2* and *4*, for the influence of the latter two is much weaker. Magnetic anomalies calculated for the model ($\Delta T_{calc.}$) were compared to magnetic anomalies reduced to the pole (RTP), used as observed data ($\Delta T_{obs.}$). Results acquired by upward continuation and

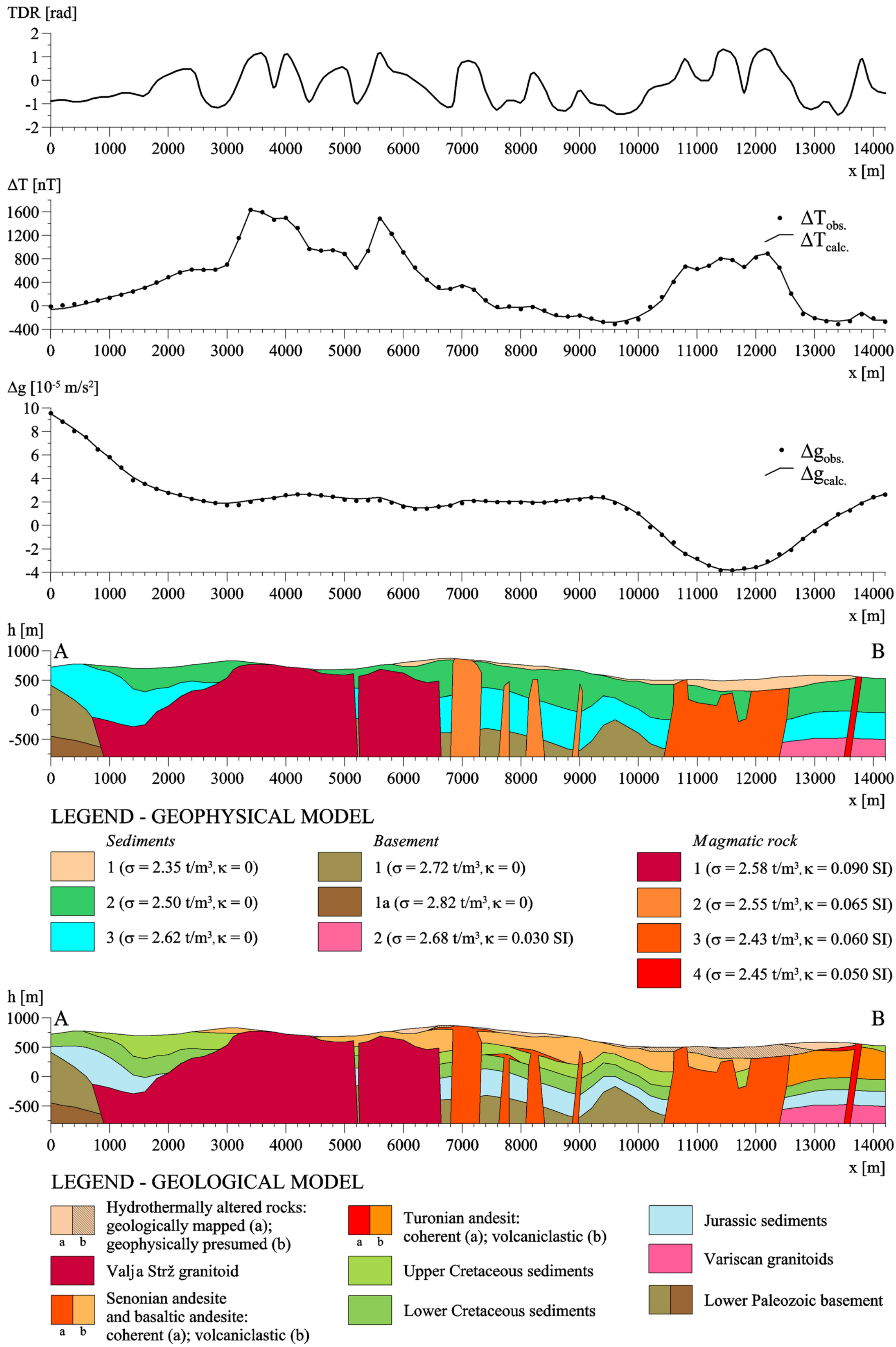
TDR [rad]
x [m]
ΔT [nT]
ΔT obs.
ΔT calc.
x [m]
Δg [10-5 m/s2]
Δg obs.
Δg calc.
x [m]
h [m]
A
B
x [m]
LEGEND - GEOPHYSICAL MODEL
Sediments
1 (σ = 2.35 t/m3, κ = 0)
2 (σ = 2.50 t/m3, κ = 0)
3 (σ = 2.62 t/m3, κ = 0)
Basement
1 (σ = 2.72 t/m3, κ = 0)
1a (σ = 2.82 t/m3, κ = 0)
2 (σ = 2.68 t/m3, κ = 0.030 SI)
Magmatic rock
1 (σ = 2.58 t/m3, κ = 0.090 SI)
2 (σ = 2.55 t/m3, κ = 0.065 SI)
3 (σ = 2.43 t/m3, κ = 0.060 SI)
4 (σ = 2.45 t/m3, κ = 0.050 SI)
h [m]
A
B
x [m]
LEGEND - GEOLOGICAL MODEL
Hydrothermally altered rocks: geologically mapped (a); geophysically presumed (b)
Valja Strž granitoid
Senonian andesite and basaltic andesite: coherent (a); volcaniclastic (b)
Turonian andesit: coherent (a); volcaniclastic (b)
Upper Cretaceous sediments
Lower Cretaceous sediments
Jurassic sediments
Variscan granitoids
Lower Paleozoic basement

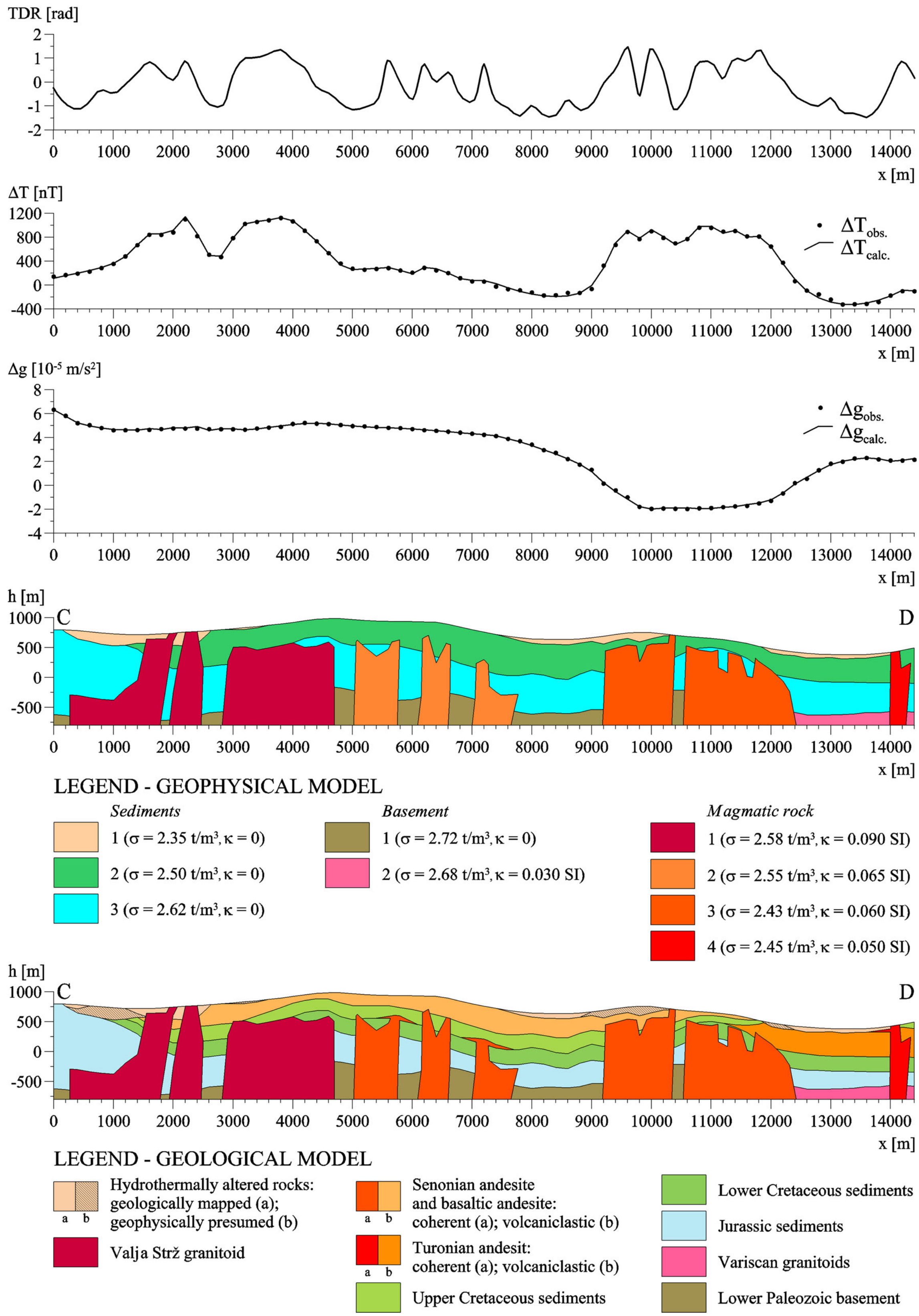

Fig. 5 2D geological–geophysical model along the section *CD* with graphics of tilt derivative (TDR), aeromagnetic anomaly (ΔT) and gravity anomaly (Δg)

upward continuation with TDR, both for levels 100 m, were considered in order to determine the basic shape of the magmatic bodies. For refining the shape and the edges of the source structures we used results of AS and TDR.

The next step in modeling was aimed at defining the spatial relationships between the inferred magmatic bodies and surrounding rocks by using the results acquired by gravity measurements. It is assumed that density of magmatic rocks differs with respect to rock types and appropriate volcanic phases. The presence of significant negative gravity anomaly confirms the extent of *magmatic rock 3* inferred from magnetic data. This implies that *magmatic rock 3* has lower density than *magmatic rock 2*, although they have similar susceptibility and most probably belong to the same volcanic phase. Sedimentary rocks were divided into three major layers of different density. *Sediments 1* correspond to low density near-surface sedimentary rocks, *sediments 2* represent clastic sediments and younger carbonates, while *sediments 3* correspond to more deeply buried carbonate rocks. The applied density values were adjusted in order to match gravity anomalies calculated for the model ($\Delta g_{\text{calc.}}$) with observed gravity anomalies ($\Delta g_{\text{obs.}}$).

The basement is the deepest high density rock unit which provides a major positive density contrast. A comparison between gravity and magnetic anomalies implies that there are generally two basement types. *Basement 1* is generally non-magnetic or very low magnetic, has higher density and corresponds to metasedimentary rocks that are similar to those occurring along the outer western margin of the TMC. However, to fit the model within the *Basement 1* we had to distinguish a sub-unit named *basement 1a* and the latter is related to variable crystallinity of the present metamorphic rocks (see below). *Basement 2* is magnetic, has lower density and corresponds to magmatic to metaigneous rocks. It is noteworthy that different values of susceptibility were appointed to *basement 2* along the modeled sections AB and CD. It is generally known that magnetic basements are often magnetically heterogeneous (Tarlowski and Koch 1988; Goussev et al. 2007).

4.2 Geological models

Geological models are given as bottom sections A–B and C–D in Figs. 4 and 5. In principle, they are derived from the above described geophysical models by upgrading them using available geological data. Accordingly, some entities of the geophysical model are divided into several rock units/series in the geological model.

One of the most striking features of the geological model is that the Valja Strž pluton has a much larger extent than it is indicated from its surface exposures (<20 km^2). According to the model, the lateral extent of the pluton at depths of $\sim$1 km is ten times larger than its surface outcrops. The pluton apparently continues towards the south and that is inferred from both sections. However, more to the south (section C–D), the pluton appears to be dismembered into three roughly subvertical intrusive branches (Fig. 5).

The model further suggests that the Santonian–Campanian volcanic rocks are also more widespread in depth than they are exposed on the surface. Both sections indicate that there are two subsurface regions of these rocks, each around 2.5–3 km in width. The western one is situated very close to the Valja Strž pluton, and is dismembered into three/four smaller bodies. The other occurrence is situated around 1.5 km more to the east and it appears more like a continuous igneous body. The modeling assumes that these two occurrences have different densities (*magmatic rocks* 2 and 3 in the geophysical model). It is generally known that the Santonian–Campanian volcanics are represented by amphibole–pyroxene andesite to basaltic andesite, which are more basic in composition than the Turonian amphibole–biotite andesite to dacite (Banješević et al. 2006; Kolb et al. 2013). Hence, the observed density differences of the two geophysically inferred bodies can be potentially explained by the relative increase in abundance of basaltic andesite toward the west. Alternatively, the eastern body could, in fact, represent multiple subvolcanic intrusions that presumably belong to both Turonian and Santonian–Campanian volcanic phase. If the latter possibility is correct, the Turonian volcanic rocks would be similar to a narrow body which presence is revealed at the easternmost side of both sections. In any case, the results of this study are in accordance with the available petrological and geological data which strongly suggest that along with the already mentioned westward progression in age, there is also a gradual westward shift in composition. This is evident from the fact that the Santonian–Campanian volcanic rocks have slightly lower silica contents than the volcanic rocks of the Turonian phase. Such compositional shift can be explained by changes in local tectonic conditions. Namely, the Santonian–Campanian phase was related to extensional tectonics in comparison to a predominantly compressive regime in the Turonian. Such extension may have been more favourable for less evolved mantle melts to reach the surface (Lips 2002; Zimmerman et al. 2008; Kolb et al. 2013).

Sediments 1 of the geophysical model partly correspond to the hydrothermally altered Santonian–Campanian andesite to basaltic andesite volcaniclastic deposits that crop out at many places in the study area. However, the model suggests that these low-density unit is more widespread in near-surface levels implying that hydrothermally altered rocks can have considerably larger distribution both horizontally and vertically. Their protoliths are most likely both Santonian–Campanian volcanic rocks and Upper Cretaceous sediments. *Sediments 2* are separated into three layers: (1) volcaniclastic rocks of the Turonian volcanic phase, (2) volcaniclastic rocks of the Santonian–Campanian volcanic phase, and (3) Upper Cretaceous carbonate and clastic sediments. *Sediments 3* correspond to Jurassic/Lower Cretaceous limestone and dolomite. The boundaries between these layers may not accurately correspond to real geological boundaries existing under the surface, but they should be used as describing the general spatial relationships between them.

Basement 1 corresponds to Lower Paleozoic metamorphic rocks, similar to those occurring more to the west of the TMC. As it is already mentioned above, the basement rocks are split into *basement 1* and *1a* in order to better fit to the geophysical model. This is in accordance to the local geology of the Palaeozoic metamorphic basement, composed of variably metamorphosed rocks ranging from low grade schists and non-metamorphosed sandstones (presumably *basement 1*), to high/medium grade gneisses and amphibolites (*basement 1a*). By contrast, *basement 2* most probably represents a westward extension of the Variscan granitoid rocks of Gornjane, which has much larger exposures eastward and north-eastward from the TMC. The influence of this granitoid is likely responsible for the complex geophysical image in the basement along the eastern margin of the TMC. It is noteworthy that the presence of Variscan granitoid rocks in the basement is also inferred from abundant dm- to m-sized fragments of these granitoids found in various volcanic rocks of the TMC (Knežević 1960; Đorđević and Banješević 1997; Banješević 2006).

5 Concluding remarks and metallogenetic implications

One of the most valuable results of this study suggests that there is a large subsurface continuation of the Valja Strž pluton towards the south. It is related to the area which has already been emphasized as very promising in terms of economically significant ore deposits (see Monthel et al. 2002). The most prospective site in the wider area is Dumitru Potok, which is situated north from the Valja Strž pluton. Our results indicate that the area south and southeast from the pluton should be also considered as prospective in terms of finding new structurally-controlled porphyry systems. It is worth noting that the limits of the southern continuation of the Valja Strž monzonite pluton are still not fully constrained, which means that the geophysical influence of this body further towards the south still remains to be unravelled by future surveys.

The Valja Strž pluton has been considered as a deeply dissected pluton (Janković 1977; von Quadt et al. 2002). It is generally accepted that such plutons are not prospective for epithermal gold mineralization since such mineralizations are usually found at shallow depths (Silitoe 1993; Hedenquist et al. 1996). However, this new evidence of relatively large masses of these intrusive rocks covered by sedimentary and volcaniclastic deposits shed new lights on this already promising area.

The model presented here also suggests that the geophysically inferred subvolcanic bodies predominantly correspond to the Santonian–Campanian volcanics. This is important because the presumed subvolcanic bodies occur in the western part of the TMC, which, in comparison to the eastern part of the complex, has long been known to have metallogenetic potential but failed to retrieve huge ore deposits. In this context, the inferred presence of covered Santonian–Campanian subvolcanic bodies must be taken into consideration in further explorations. Furthermore, the model also indicates that it is not likely that larger masses of Turonian volcanic occur underneath the western TMC.

Another significant implication is related to larger shallow occurrences of hydrothermally altered rocks, which are also revealed by our geophysical data. It has been already known that hydrothermally altered rocks are more widespread in the western parts of the TMC, i.e. in the area dominated by the Santonian–Campanian volcanic and volcaniclastic rocks, although this area lacks very large and economically significant ore bodies (Banješević 2006; Koželj 2002). The geophysically inferred near-surface hydrothermally altered rocks are particularly abundant above the eastern occurrence of subsurface coherent magmatic bodies and this suggests that this area can also be very promising for further explorations.

The outcomes of this study strongly suggest that there is a great need for further investigations throughout the TMC and along its outer periphery. The approaches integrating geophysical surveys and detailed geological/petrological studies can be particularly fruitful. It is so, because only interdisciplinary research has potential of improving the existing predictive exploration models.

Acknowledgements This study was supported by the Serbian Ministry of Education, Science and Technological Development (Projects Nos. 176016 and 33003). Special support was provided by the SCOPES Project (IZ73Z0-128089) funded by the Swiss National Science Foundation, which covered most of field expenses. CV thanks to the Serbian Academy of Sciences and Arts (Project Geodynamics).

References

Andrić, B., Antonijević, I., Grubić, A., Dragašević, T., Đorđević, M., & Terzić M. (1972). Analiza građe Timočkog rov-sinklinorijuma u svetlosti novih geoloških i geofizičkih istraživanja. *III*

Savetovanje o istraživanju bakrove mineralizacije na teritoriji SFRJ, Bor, p. 16.

Antonijević, A., & co-authors. (1968). Basic geological map of SFRY 1:100.000, Sheet Žagubica L 34-140. Belgrade: Federal Geological Institute.

Antonijević, A., & co-authors. (1974). Basic geological map of SFRY 1:100.000, Sheet Bor L 34-141. Belgrade: Federal Geological Institute.

Antonijević, I., Grubić, A., & Đorđević, M. (1974). The Upper Cretaceous paleorift in eastern Serbia. In S. Karamata (Ed.), *Metallogeny and concept of the geotectonic development of Yugoslavia* (pp. 315–339). Faculty of Mining and Geology: Belgrade.

Banješević, M. (2006). Gornjokredni magmatizam Timočkog magmatskog kompleksa. *Ph.D. dissertation*, University of Belgrade (184 pp). Belgrade: Faculty of Mining and Geology.

Banješević, M., Cocić, S., & Radović, M. (2001). Petrology and K/Ar ages of volcanic rocks for widen Bor zone as the part of the Timok Magmatic Complex (East Serbia). *ABCD GEODE Workshop*, Vata Bai, Romania, Abstract, pp. 39.

Banješević, M., Cvetković, V., Koželj, D., Peytcheva, I., & von Quadt, A. (2002). The Timok Magmatic Complex and Ridan Krepoljin Zone: Geodynamical Evolution. In: D. Koželj, & R. Jelenković (Eds.), *International Symposium—Geology and metallogeny of copper and gold deposits in the Bor metallogenic zone—Bor 100 years* (pp. 199–202), Special issue, RTB Bor Holding Company.

Banješević, M., Cvetković, V., von Quadt, A., Peytcheva, I., Cocić, S. (2006). Geodynamic reconstructions based of the magmatism in the Timok magmatic complex (east Serbia)—part of the Carpathian-Balkan belt. *XVII Congress CBGA*. Belgrade, Serbian Geological Society, Abstracts pp. 27–29.

Berza, T., Constantinescu, E., & Serban-Nicolae, V. (1998). Upper Cretaceous magmatic series and associated mineralisation in the Carpathian-Balkan Orogen. *Resource Geology, 48*, 291–306.

Blakely, J. R. (1995). *Potential theory in gravity and Magnetic application* (441 pp.). Cambridge: Cambridge University Press.

Ciobanu, C., Cook., Stein H. (2002). Regional setting and geochronology of the Late Cretaceous Banatitic Magmatic and Metallogenetic Belt. Mineralium Deposita, *37*, 541–567.

Clark, H. A., & Ullrich, D. T. (2004). ^{40}Ar/^{39}Ar age data for andesitic magmatism and hydrothermal activity in the Timok Massif, eastern Serbia: Implications for metallogenetic relationships in the Bor copper-gold subprovince. *Mineralium Deposita, 39*, 256–262.

Cassinis, G. (1930). Sur l'adoption d'une formule internationale pour la pesanteur normale. *Bulletin Géodésique*, *26*, 40–49.

Cooper, G. R. J., & Cowan, D. R. D. (2005). Differential reduction to the pole. *Computer & Geosciences, 31*, 989–999.

Cooper, G. R. J., & Cowan, D. R. D. (2006). Enhancing potential field data using filters based on the local phase. *Computer & Geosciences, 32*, 1585–1591.

Đorđević, M., & Banješević, M. (1997). *Geologija južnog dela Timočke eruptivne oblasti, Tumač i geološka karta 1:50000* (p. 171). Savezno Ministarstvo za privredu: Beograd.

Goussev, S. A., Pierce, J. W., Egorov, V. I. (2007). Magnetic basement: Gravity guided magnetic source depth analysis and interpretation. *EGM 2007 International Workshop Innovation in EM, Grav and Mag Methods: A new Perspective for Exploration*, Capri, Italy, April 15–18, 2007.

Hedenquist, J. W., Izawa, E., Arribas, A. (1996). Epithermal gold deposits: Style, characteristics and exploration. *Society of Resource Geology of Japan*, Special Publication 1, pp. 32.

Janković, S. (1977). The copper deposits and geotectonic setting of the Tethyan Eurasian Metallogenetic Belt. *Mineralium Deposita, 12*, 37–47.

Janković, S. (1990). Types of copper deposits related to volcanic environment in the Bor district, Yugoslavia. *Geologische Rundschau, 79*, 467–478.

Janković, S., Jelenković, R., Koželj D. (2002). *Borsko ležište bakra i zlata—The Bor Copper and Gold Deposit* (298 pp.), On the occasion of 100 years since discovery Bor ore deposit, Bor Lake, RTB Bor Holding Company.

Karamata, S., Knežević, V., Pécskay, Z., & Đorđević, M. (1997). Magmatism and metallogeny of the Ridanj-Krepoljin belt (Eastern Serbia) and their correlation with northern and eastern analogues. *Mineralium Deposita, 32*, 452–458.

Knežević, V. (1960). Granitski odlomci u vulkanskim brečama kod Brestovačke Banje i Bora. *Zbornik Rudarsko-geološkog fakulteta, 6*, 107–113.

Kolb, M., von Quadt, A., Peytcheva, I., Heinrich, C. A., Fowler, S. J., & Cvetković, V. (2013). Adakite-like and normal arc Magmas: Distinct fractionation paths in the East Serbian segment of the Balkan-Carpathian Arc. *Journal of Petrology, 54*, 421–451.

Koželj, D. (2002). Epitermalna mineralizacija zlata Borske metalogenetske zone. Morfogenetski tipovi, strukturno-teksturni varijeteti i potencijalnost (219 pp.). On the occasion of 100 years since discovery Bor ore deposit, Bor Lake, RTB Bor Holding Company.

Koželj, D., & Jelenković, R. (2001). Ore forming environments of epithermal gold mineralization in the Bor metallogenetic zone, Serbia, Yugoslavia. *6th Biennial SGA Meeting*, Krakow, pp. 535–538.

Krstić, B., & Karamata, S. (1992). Terrranes of the Eastern Serbian Carpatho-Balkanides. *Comptes rendus des Seances de la Société Serbe de Géologie, Livre Jubilaire (1981–1991)*, pp. 57–74.

Li, X. (2008). Magnetic reduction-to-the-pole at low latitudes: Observations and considerations. *The Leading Edge, 27*, 990–1002.

Lips, A. (2002). Correlating magmatic–hydrothermal ore deposit formation over time with geodynamic processes in SE Europe. In: D. Blundell, F. Neubauer & A. von Quadt (Eds.), *The timing and location of major ore deposits in an evolving orogen* (pp. 69–79). *Geological Society of London, Special Publications 204.*

Lips, A., Herrington, R. J., Stein, G., Koželj, D., Popov, K., & Wijbrans, J. R. (2004). Refined timing of porphyry copper formation in the Serbian and Bulgarian portions of the Cretaceous Carpatho-Balkan Belt. *Economic Geology, 99*, 601–609.

Ljubović-Obradović, D., Carevac, I., Mirković, M., & Protić, N. (2011). Upper Cretaceous volcanoclastic-sedimentary formations in the Timok Eruptive Area (eastern Serbia): new biostratigraphic data from planktonic foraminifera. *Geologica Carpathica, 62*, 435–446.

Luyendyk, A. P. J. (1997). Processing of airborne magnetic data. *Journal of Australian Geology & Geophysics, 17*, 31–38.

Mitchell, A. H. G. (1996). Distribution and genesis of some epizonal Zn/Pb and Au provinces in the Carpathia-Balkan region. *Transactions of the Institution of Mining and Metallurgy Section B, 105*, 127–138.

Monthel, J., Vadala, P., Leistel, J. M., Cottard, F., Ilić, M., Štrumberger, A., Tošović, R., Stepanović, A. (2002). Mineral deposits and mining districts of Serbia. *Compilation map and GIS databases. BRGM/RC-51448-FR*, 67 pp.

Nabigian, M. N. (1972). The analytic signal of two-dimensional magnetic bodies with polygonal cross-section: its properties and use for automated anomaly interpretation. *Geophysics, 37*, 507–517.

Pačevski, A., Götzinger, M., Dimitrijević, R., & Cvetković, L. (2007). Oscillatory zoning in wolframite from Osanica, near Bor, Serbia. *Neues Jahrbuch für Mineralogie Abhandlungen, 184*, 151–160.

Pačevski, A., Libowitzky, E., Živković, P., Dimitrijević, R., & Cvetković, L. (2008). Copper-bearing pyrite from the Čoka

Marin polymetallic deposit, Serbia: Mineral inclusions or true solid-solution? *Canadian Mineralogist, 46*, 249–261.

Pačevski, A., Moritz, R., Kouzmanov, K., Marquardt, K., Živković, P., & Cvetković, L. (2012). Texture and composition of Pb-bearing pyrite from the Čoka Marin polymetallic deposit, Serbia, controlled by nanoscale inclusions. *Canadian Mineralogist, 50*, 1–20.

Salem, A., Williams, S., Fairhead, J. D., Ravat, D., & Smith, R. (2007). Tilt-depth method: A simple depth estimation method using first-order magnetic derivatives. *The Leading Edge, 26*, 1502–1505.

Săndulescu, M. (1984). *Geotectonics of Romania* (336 pp.). Bucuresti: Editura Tehnica.

Schmid, S. M., Bernoulli, D., Fügenschuh, B., Matenco, L., Schefer, S., Schuster, R., et al. (2008). The Alpine-Carpathian-Dinaridic orogenic system: correlation and evolution of tectonic units. *Swiss Journal of Geosciences, 101*, 139–183.

Silitoe, R. H. (1993). Epithermal models: genetic types, geometrical controls and shallow features. *Mineral Deposit Modelling. Geological Association of Canada, Special Paper, 40,* 403–417.

Stoykov, S., Peytcheva, I., von Quadt, A., Moritz, R., Frank, M., & Fontignie, D. (2004). Timing and magma evolution of the Chelopech volcanic complex (Bulgaria). *Schweizerische Mineralogische und Petrographische Mitteilungen, 84*, 101–117.

Tarlowski, C., & Koch, I. (1988). On the problem of estimating the depth to the magnetic basement. *Geophysics, 53*, 1362–1363.

Vasković, N., Belousova, E., O'Reilly, S. Y., Griffin, W. L., Srećković-Batoćanin, D., Christofides, G. & Koroneos, A. (2012). New U-Pb dating and Hf-isotope composition of the Gornjane granitoids (South Carpathians, East Serbia). *Acta Mineralogica-Petrographica, Abstract Series, Szeged*, *7*, 146.

von Quadt, A., Ivanov, Z. & Peytcheva, I. (2001). The Central Srednogorie (Bulgaria) part of the Cu (Au–Mo) belt of Europe: A review of the geochronological data and the geodynamical models in the light of the new structural and isotopic studies. In A. Piestrzynski, (Ed.), *Mineral Deposits at the Beginning of the 21st Century*, Proceedings of the Joint Sixth Biennial SGA-SEG Meeting, Krakow (pp. 555–558).Tokyo: A.A. Balkema Publishers.

von Quadt, A., Moritz, R., Peytcheva, I., & Heinrich, C. (2005). Geochronology and geodynamics of Late Cretaceous magmatism and Cu–Au mineralization in the Pangyurishte region of the Apuseni–Banat–Timok–Srednogorie belt, Bulgaria. *Ore Geology Reviews, 27*, 95–126.

von Quadt, A., Peytcheva, I., Cvetković, V., Banješević, M., & Koželj, D. (2002). Geochronology, geochemistry and isotope tracing of the Cretaceous magmatism of East-Serbia as part of the Apuseni–Timok–Srednogorie metallogenic belt. *Geologica Carpathica, 53*, 175–177.

von Quadt, A., Peytcheva, I. & Heinrich, C. (2007). Upper Cretaceous magmatic evolution and related Cu–Au mineralization in Bulgaria and Serbia. In: C. J., Andrew (Ed.), *Nineth Biennial Meeting of the Society for Geology Applied to Mineral Deposits SGA, Dublin* (pp. 861–864). Dublin: Irish Association for Economic Geology.

von Quadt, A., Peytcheva, I., Heinrich, C. A., Frank, M., & Cvetković, V. (2003). Evolution of the Cretaceous magmatism in the Apuseni–Timok–Srednogorie metallogenic belt and implications for the geodynamic reconstructions: new insight from geochronology, geochemistry and isotope studies. *EGS-AGU-EUG Joint Assembly, 1*, 9219.

Zimmerman, A. (2006). Tectonic configuration of the Apuseni–Banat–Timok–Srednogorie Belt, Southeastern Europe, constrained by high precision Re–Os molybdenite ages. *M.S. Thesis*, Colorado State University, 91 pp.

Zimmerman, A., Stein, H. J., Hannah, J. L., Koželj, D., Bogdanov, K., & Berza, T. (2008). Tectonic configuration of the Apuseni–Banat–Timok–Srednogorie belt, Balkans-South Carpathians, constrained by high precision Re/Os molybdenite ages. *Mineralium Deposita, 43*, 1–21.